KfK 3105
Januar 1982

104 MeV Alpha Particle Scattering from ^{90,92}Zr

V. Corcalciuc, H. J. Gils, H. Rebel, J. Buschmann,
R. Pesl, R. Dumitrescu, S. Zagromski, K. Feißt
Institut für Angewandte Kernphysik

Kernforschungszentrum Karlsruhe

KERNFORSCHUNGSZENTRUM KARLSRUHE

Institut für Angewandte Kernphysik

KfK 3105

104 MeV ALPHA PARTICLE SCATTERING FROM $^{90,92}Zr$

V. Corcalciuc*, H.J. Gils, H. Rebel, J. Buschmann, R. Pesl,
R. Dumitrescu*, S. Zagromski, and K. Feißt

Kernforschungszentrum Karlsruhe GmbH, Karlsruhe

*Institute for Physics and Nuclear Engineering,
Bucharest, Romania

Kernforschungszentrum Karlsruhe GmbH
ISSN 0303-4003

ABSTRACT

Differential cross sections have been measured for the elastic and inelastic scattering of 104 MeV alpha-particles from $^{90,92}Zr$. The experimental data are analyzed in terms of coupled channels on the basis of a flexible anharmonic vibrator model and using different parametrizations of the radial shape of the extended optical potential. The results favour the squared Saxon-Woods type for the real part. Additionally to a radial momentum analysis of the real potentials a semimicroscopic folding model has been applied for extracting isoscalar quadrupole and hexadecapole transition rates.

ZUSAMMENFASSUNG

Streuung von 104 MeV Alphateilchen an $^{90,92}Zr$

Die differentiellen Wirkungsquerschnitte für die elastische und unelastische Streuung von 104 MeV Alphateilchen an $^{90,92}Zr$ wurden gemessen. Die experimentellen Daten wurden mit der Methode der gekoppelten Kanäle auf der Basis eines flexiblen anharmonischen Vibrationsmodells und mit verschiedenen Parametrisierungen der radialen Form des deformierten optischen Potentials analysiert. Die Resultate favorisieren die quadratische Saxon-Woods-Form für den Realteil. Neben der Analyse der radialen Momente der Potentiale wurde ein halbmikroskopisches Faltungsmodell benutzt, um isoskalare Quadrupol- und Hexadekapol-Übergangsraten zu gewinnen.

1. INTRODUCTION

For a long time alpha-particle scattering is known to be important and well-established tool for studies of the general mechanism of reactions between complex nuclear particles and for exploring interesting nuclear structure properties. In recent years, there has been a considerable progress (see ref. 1) which is due to (i) an increased precision of the measurements, in particular at higher alpha-particle energies, (ii) an improved understanding of the reaction mechanism[2,3] (also in terms of a microscopic description), and due to (iii) more refined methods[4,5,6] for the theoretical analysis of the experimental cross sections. The recent methods do not only overcome some restrictions and constraints of earlier procedures, they are also able to reveal small isotopic variations of the radial shapes of the optical potentials (reflecting those of the underlying matter distributions).

One of the more general results of recent elastic alpha-particle scattering investigations shows that the overall radial shape of the real part of the alpha-particle scattering optical potential is significantly better represented by a squared Saxon-Woods-form (SW2) rather than by the standard Saxon-Woods (SW) parametrization[7,8]. These phenomenological findings can be justified by the folding model approach[9] generating the real part of the optical potential by a convolution of the nuclear matter distribution and an effective alpha-particle-bound nucleon interaction. The question, however, whether the phenomenological squared Saxon-Woods form has to be extended also to the shape of (permanently or dynamically) deformed optical potentials is not sufficiently investigated (see e.g. in ref. 16). The collective model provides the radial form factors for the nuclear excitation induced by scattering as derivatives of the radial shape of the diagonal optical potential (mainly determined by the elastic scattering alone). All procedures[9] for extracting isoscalar transition rates from inelastic alpha-particle scattering basically rely on the particular parametrization of the transition potentials. In view of the interest in comparing consistently the strengths of electromagnetic, (p,p') (π,π') and (α,α') excitations which involve proton and neutron transition matrix elements in a different way, it seems worthwhile to study to which extent different

alternative models influence the theoretical descriptions of the experimental results and how they affect the extracted values of the transition rates.

In this paper we report on experimental studies of 104 MeV alpha-particle scattering from low-lying levels of $^{90,92}Zr$. The elastic alpha-particle scattering from the Zr isotopes has been already extensively studied by several authors[6,8,10,14] using different improved parametrizations of the optical potential. Therefore, this particular case appears quite adequate to proceed to more detailed studies of the deformed optical potential by inelastic scattering. The measured elastic and inelastic differential cross sections are the basis of extensive coupled channel calculations specifying the transition potentials in terms of a somewhat generalized (rather flexible anharmonic) vibrator model[11]. Such a description includes also the possibility of direct hexadecapole transitions to the 4^+_1 states. In addition to studies of the shape of the transition potentials the determination of B(I4) values presents a further motivation and is of particular interest for the discussion of a possible hexadecapole motion in spherical nuclei[12], core excitation models and coupling to giant hexadecapole states. Additionally, to the analysis on the basis of a phenomenologically deformed interaction potential a semi-microscopic folding model is invoked for deducing the deformed optical potential from a deformed nucleon distribution. The values of the isoscalar transition rates as found by the various alternative procedures are discussed.

2. EXPERIMENTALS

The measurements of the differential cross sections of alpha-particle scattering from the groundstates, 2^+_1 and 4^+_1 levels of $^{90,92}Zr$ used the 104 MeV alpha-particle beam and the scattering facilities at the Karlsruhe Isochronous Cyclotron. The targets were self-supporting foils of 3,8 mg/cm² (^{90}Zr) and 4.5 mg/cm² (^{92}Zr), respectively. The alpha-particle beam was monochromized in energy to about 60 keV. The energy spectra of the scattered alpha-particles were measured by four 4 mm thick silicon surface barrier detectors rigidly mounted to the same movable arm with a fixed angular distance between each other of 1.5°. The overall energy resolution was approximately 150-200 keV FWHM. Particle

identification was found not to be necessary due to the large negative Q-values of $(\alpha,{}^{3}He)$ reactions and the large differences in the energy loss of light ejectiles (p,t) transversing the silicon detectors. In the forward scattering angles spectra there are contamination peaks from ^{12}C and ^{16}O which beyond $\Theta_{Lab} \gtrsim 30°$ walk out of the region of interest. In detailed analyses of the energy spectra the line shapes were fitted by an asymmetric Gaussian form and a continuous background. The differential cross sections were taken in steps of 0.5° in a laboratory angular range from 7°-54° for ^{92}Zr, up to ca. 70° for ^{90}Zr. The angular distributions have a good angular accuracy ($\Delta\Theta \gtrsim 0.2$) due to a relatively large scattering chamber (Ø = 130 cm) a small beam spot and a beam divergence of ca. 0.1°. The absolute zero of the angular scale has been determined by measuring sharp diffraction minima on both sides of the incident beam. The quoted errors include the uncertainty due to the finite angular acceptance (transformed into cross section errors). Considering the uncertainties of the target thickness, the detector solid angle and of the integrated beam current the absolute scale of the cross sections is determined within ca. 10%.

3. ELASTIC SCATTERING

Our studies of elastic scattering are looking for some indications of isotope differences in alpha-particle scattering from ^{90}Zr and ^{92}Zr. In Fig. 1 the measured elastic cross sections are displayed (together with theoretical curves explained below). In the lower part the quantity

$$\frac{d\sigma/d\Omega(^{92}Zr)-d\sigma/d\Omega(^{90}Zr)}{d\sigma/d\Omega(^{92}Zr)+d\sigma/d\Omega(^{90}Zr)} \qquad (3.1)$$

vs. C.M. scattering angle is plotted indicating a slightly increased size of ^{92}Zr. A detailed analysis should apply one of the recently introduced "model-independent" procedures, e.g. the Fourier-Bessel method[4] which avoids constraints due to a pre-chosen simple function form of the shape of the optical potential and additionally provides realistic estimates of the uncertainties (Details of the method and a demonstration of the procedures are given in ref. 4 and 13). A reasonable application of the

Fourier-Bessel method, however, requires sufficiently precise data extending beyond the diffraction region. Unfortunately, the measured ^{92}Zr data prove to be not of the required quality so that a Fourier-Bessel analysis has been performed only for the ^{90}Zr case. Fig. 2 shows the resulting (real) Fourier-Bessel potential and demonstrates that the SW2 form is a good overall substitute. The values of the best-fit parameters (depth V_0, half way radius $r_v A^{1/3}$ and surface diffuseness a_v), the volume integrals per nucleon pair ($J_0/4A$) and of the goodness of the fits, χ^2 per degree of freedom, are compiled in Table 1 for the SW as well as for the SW2 parametrization. In all cases the imaginary part of the optical potential was parametrized by the usual SW shape (W_0, $r_w A^{1/3}$ and a_w) for which some arguments are given in ref. 14. The optical model calculations used the computer code MODINA[15].

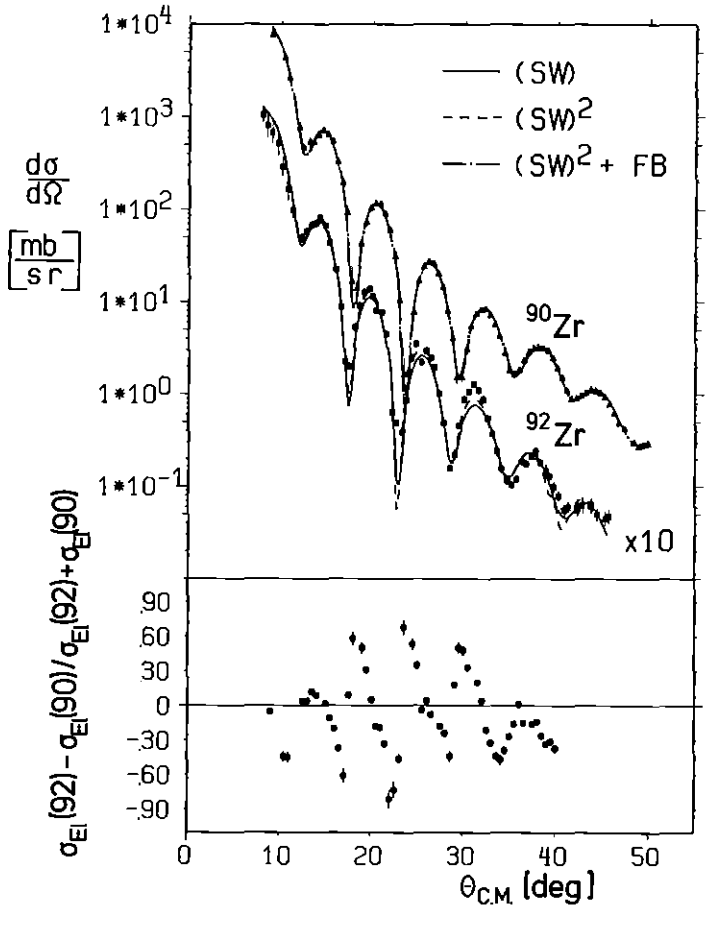

Fig. 1
Elastic scattering of 104 MeV alpha-particles from $^{90,92}Zr$ and optical model calculations with different radial shapes of the real part: Saxon-Woods (SW) form - squared Saxon-Woods form (SW2)-Fourier-Bessel-potential (FB).
The lower part displays the relative difference of the differential cross sections for $^{90,92}Zr$.

	V_o (MeV)	r_v (fm)	a_v (fm)	W_o (MeV)	r_w (fm)	a_w (fm)	$J_o/4A$	χ^2/F
^{90}Zr SW	131.1	1.255	0.766	21.09	1.55	0.62	321.4	3.95
SW2	165.1	1.354	1.276	20.84	1.54	0.64	307.1	2.48
FB				22.60	1.44	0.86	289.7	1.25
^{92}Zr SW	126.3	1.24	0.845	21.7	1.57	0.67	311.1	7.22
SW2	151.6	1.37	1.397	18.95	1.62	o.615	293.4	5.22

Table 1 Optical potentials for $^{90,92}Zr(\alpha,\alpha)^{90,92}Zr$ at E_α = 104 MeV

SW: $V_o \cdot f(r_\alpha) + i\, W_o\, g(r_\alpha)$

SW2: $V_o (f(r_\alpha))^2 + i\, W_o\, g(r_\alpha)$

FB: Real Fourier-Bessel potential + $i\, W_o\, g(r_\alpha)$

with $f(r_\alpha) = \{1 + \exp((r_\alpha - r_v \cdot A^{1/3})/a_v)\}$

and $g(r_\alpha) = \{1 + \exp((r_\alpha - r_w \cdot A^{1/3})/a_w)\}$

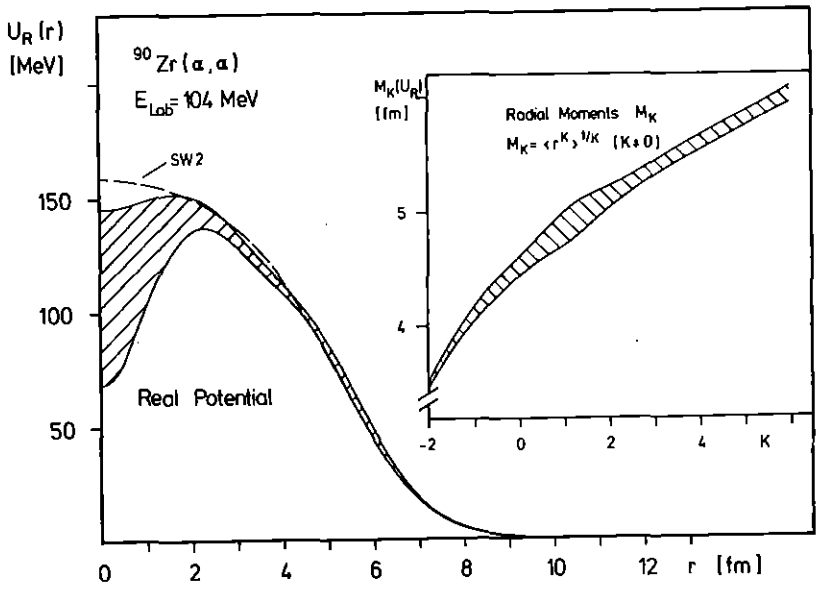

Fig. 2 The real part of the (α+^{90}Zr) optical potential: Result of the Fourier-Bessel method compared to the best-fit SW2 potential (hatched area represents the error band of the FB-potential). The inset shows the values of the radial moments M_K and their uncertainties.

4. INELASTIC SCATTERING

In the framework of the collective model the non-diagonal part U_{coupl} of the complex interaction potential providing the coupling of different nuclear states is deduced from an extended optical potential

$$U(\vec{r}_\alpha) = -V_o f(\vec{r}_\alpha) - i\, W_o\, g(\vec{r}_\alpha) \ , \qquad (4.1)$$

deformed by the angular dependence of the half-way radius. e.g.

$$R\,(\hat{r}_\alpha) = R_o\,(1 + \sum \alpha_{\lambda_\mu}\, Y_{\lambda\mu}(\hat{r}_\alpha)) \qquad (4.2)$$

and expanded into powers (t) of $\sum_{\lambda\mu} \alpha_{\lambda_\mu}\, Y_{\lambda\mu}(\hat{r}_\alpha)$

The coupling between various channels is given by the matrix elements

$$\langle \ell I | U_{coupl} | \ell' I' \rangle = \sum_L A(\ell, I, \ell' I', LJ) \cdot \sum_t u_L^{(t)}(r)\ \langle I || Q_L^{(t)} || I' \rangle \qquad (4.3)$$

where the factors $A(\ell, I, \ell' I', LJ)$ (depending on the partial waves of the incoming (ℓ) and scattered (ℓ') particles, the nuclear spins I,I', the channel spin J and multipolarity L) are purely geometrical. The reduced matrix elements of the operators $Q_L^{(t)}$ (operating only on target coordinates and built up by the α_λ-operators coupled to the multipolarity L) determine the strength of the transitions while the radial form factors $u_L^{(t)} = v_L^{(t)} + i\, w_L^{(t)}$ are defined as derivatives (t) of the shapes $f(r_\alpha)$ and $g(r_\alpha)$.

We restrict our consideration to the case of a coupling of the low lying states 0^+, 2^+_1 and 4^+_1, and to the second order: t = 2. Then, we have to consider the following matrix elements ("deformation parameters")[11]

(i) Single step quadrupole transitions (4.5)

$$\langle 0 || Q_2^{(1)} || 2^+_1 \rangle = \beta_{02}$$

$$\langle 2_1 || Q_2^{(1)} || 4^+_1 \rangle = \beta_{24}\, \sqrt{\frac{18}{5}}$$

(ii) Single step hexadecapole transition:

$$\langle 0||Q_4^{(1)}||4_1\rangle = \beta_{04}$$

(iii)Two-step hexadecapole transition

$$\langle 0||Q_4^{(2)}||4_1\rangle = \beta_{04}^{2'}\langle 2200|40\rangle / \sqrt{2\pi}$$

We do not use the simplifications of a harmonic quadrupole vibrator model

$$\beta_{02} = \beta_{24} = \beta'_{04} = \beta_2 \qquad (4.5a)$$
$$\beta_{04} = 0$$

and take β_{02}, β_{24} and β_{04} as free parameters (and $\beta'_{04} = \sqrt{\beta_{02}\,\beta_{24}}$) so that there is a flexible way (anharmonic vibrator model) to specify independently the strengths of different transitions. In fact, the model dependence is considerably reduced and the anharmonic vibrational model works just as a convenient formalism covering quite general cases. In contrast to the DWBA which takes into account only the couplings to the groundstate, the coupled channel calculations include automatically the competition of various excitation paths. In general, the real as well as the imaginary part of $U(\vec{r}_\alpha)$ are assumed to be nonspherical. Complex coupling proves to be important for inelastic alpha-particle scattering. In the following calculations the imaginary part of $U(r_\alpha)$ is described in the traditional manner by a deformed Saxon-Woods shape with a geometry ($g(\vec{r}_\alpha, R_w, a_w)$) independent from the real part. Table 2 compares the results (best fits to the experimental cross sections) obtained with the two different alternatives of $f(r_\alpha)$. The SW2 form proves to be generally superior, not only for the diagonal potential, but also for describing the inelastic excitations (compare partial χ^2/F). The values of the two deformation parameters β_{02} and β_{04} are rather sensitively determined by the experimental data (β_{24} proves to be less sensitive) and do not significantly differ in both approaches. The improvement

seems to be due to the somewhat modified shape of the transition potentials (see Fig. 3). For the coupled channel calculations the Karlsruhe version of the code ECIS [17] has been used.

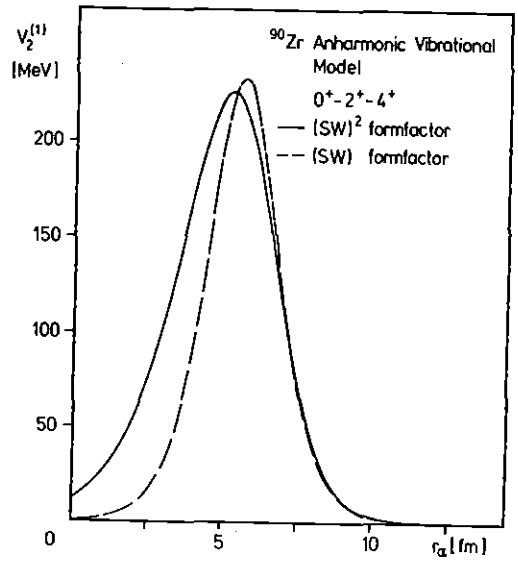

Fig. 3 Comparison of first order radial form factors as found by the coupled channel analysis of the differential cross sections for $^{90}Zr(\alpha,\alpha')$ scattering.

There is considerable interest[26,27] in comparing electromagnetic nuclear excitation (involving isovector as well as isoscalar components) and isoscalar excitation of the total nucleon distribution as induced by (α,α') scattering. However, it is by no means clarified in which way the deformation parameters of the complex interaction potential are related to the corresponding quantities of the nucleon distribution of the probed target nucleus. An "extended" folding model has been proposed[18] in order to disentangle the properties of the probing alpha-particle and of the probed target nucleus. The procedure essentially consists in writing the real part of the extended optical potential (eq. 4.1) by folding an effective alpha-particle-bound nucleon interaction $V_{eff}(r_\alpha, r)$ over a deformed Fermi nucleon distribution $\rho(\vec{r})$

Target	Shape	V_o (MeV)	r_v (fm)	a_v (fm)	W_o (MeV)	r_w (fm)	a_w (fm)	β_{02} ($1o^{-2}$)	β_{04} ($1o^{-2}$)	β_{24} ($1o^{-2}$)	$J_o/4A$ (MeV fm^3)	χ^2_t/F	χ^2_0/F	χ^2_{2+}/F	χ^2_{4+}/F
^{90}Zr	SW	128.9	1.25	0.77	20.3	1.55	0.62	6.0±0.2	2.8±0.3	0.43±0.1	301.2	3.8	3.6	7.4	2.9
	SW2	159.2	1.36	1.27	19.8	1.54	0.64	6.3±0.3	2.2±0.3	1.4±0.4	299.8	4.8	4.4	7.1	3.2
^{92}Zr	SW	121.3	1.24	0.85	20.3	1.57	0.67	8.2±0.4	3.0±0.3	.7 ±0.3	296.6	10.0	10.0	15.8	3.0
	SW2	153.3	1.36	1.42	18.5	1.63	0.56	6.0±0.3	2.6±0.3	2.4±0.5	288.6	7.0	8.0	8.72	3.3

Table 2 $^{90,92}Zr(\alpha,\alpha')$: Extended optical potential with SW and SW2 radial shapes.

Target	W_o (MeV)	r_w (fm)	a_w (fm)	β_{02} ($1o^{-2}$)	β_{04} ($1o^{-2}$)	β_{24} ($1o^{-2}$)	χ^2_t/F	χ^2_0/F	χ^2_{2+}/F	χ^2_{4+}/F
^{90}Zr	27.3	1.44	0.705	8.6±0.5	5.5±0.5	5.0±0.8	18.4	46.6	9.1	1.9
^{92}Zr	27.5	1.47	0.705	10±0.4	5.0±0.6	6.4±0.9	10.2	15.2	7.0	2.5

Table 3 $^{90,92}Zr(\alpha,\alpha')$: Results of the folding model procedure

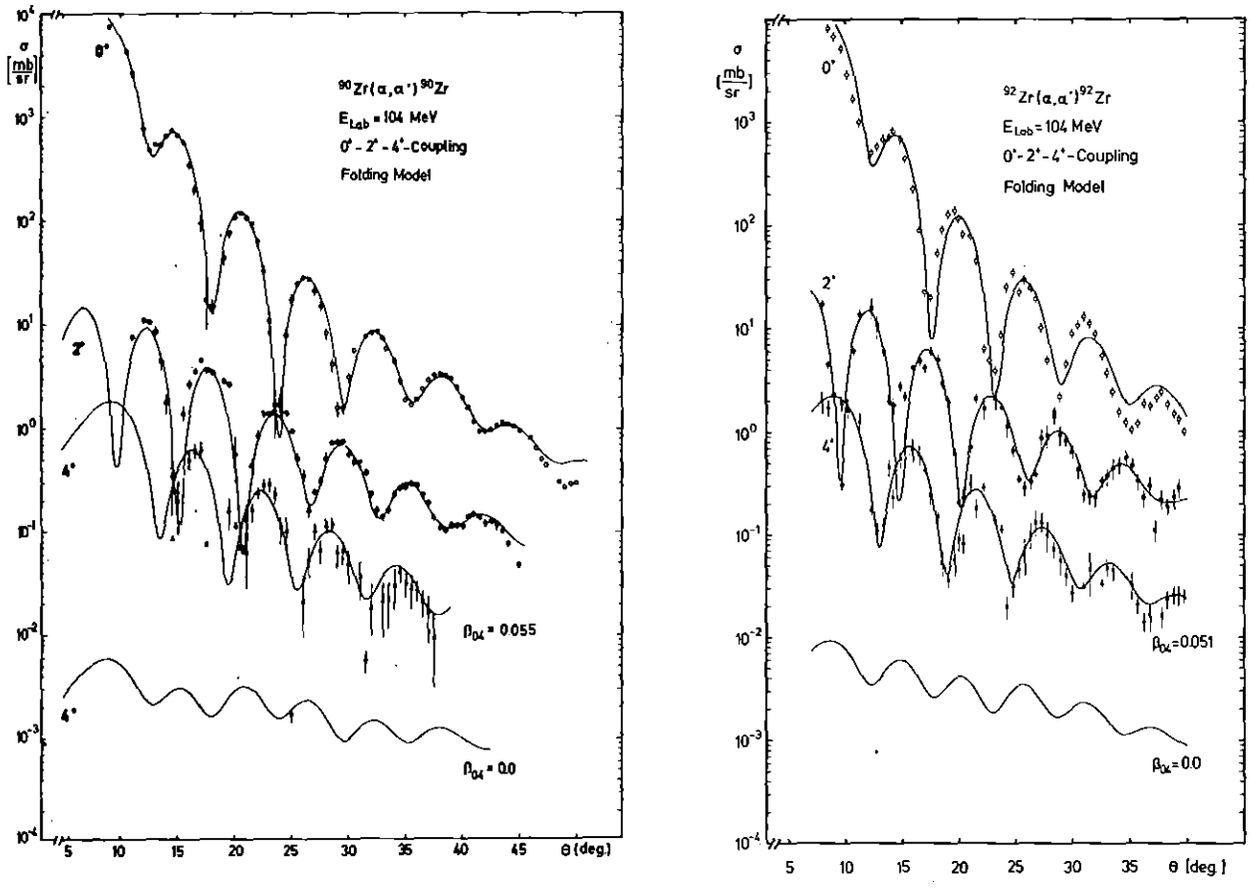

Fig. 4 $^{90,92}Zr$ (α,α') : Experimental differential cross sections and results of the theoretical analysis on the basis of a deformed folding model for the real part of the optical potential.

$$V(\vec{r}_\alpha) = \int V_{eff}\,(r_\alpha,\, r)\rho(\vec{r})\; d^3r \qquad (4.6)$$

The approach has been successfully applied in several cases (see for example ref. 19,20). A simple Gaussian form is chosen for the effective interaction

$$V_{eff}(r_\alpha,r) = -\lambda_R\, V_0 \exp\,[-[\vec{r}-\vec{r}_\alpha]/\mu_0{}^2] \qquad (4.7)$$

where V_0 = -40 MeV and μ_0 = 1.95 are derived folding the effective nucleon-nucleon interaction over the alpha-particle density distribution, and λ_R = 0.996 is a parameter adjusted[20] by elastic alpha-particle scattering on ^{40}Ca and absorbing some uncontrolled uncertainties.

The deformation of $\rho(\vec{r})$ is introduced (similarity to eq. 4.2) by the angular dependence of the half way radius.

$$c_m(\hat{r}) = c_o \left(1 + \sum \alpha_{\lambda\mu} Y_{\lambda\mu}(\hat{r})\right) \qquad (4.8)$$

The value of c_o and of the surface diffuseness a_m of the Fermi distribution are taken from electron scattering results (c_o = 1.06 fm, a_m = 0.5 fm and 0.63 fm for ^{92}Zr, respectively). When fitting the experimental cross sections only the (phenomenologically parametrized) imaginary part and the "matter deformation parameters" (corresponding to the matrix elements given by eqs. 4.5) are adjusted (see Table 3). Though the resulting χ^2/F values are obviously larger than in the phenomenological approach, we observe again the not unexpected effect of increased values of the "matter deformation" as compared to the "potential deformation". Recent elastic alpha-particle scattering studies have shown[3] that a density-dependent effective interaction V_{eff} is required when the data extend to larger angles beyond the diffraction region. A density independent effective interaction and the neglect of exchange effects are limits of the present folding approach in describing the data. Moreover, it should be noted that there is a difference in handling the complex coupling in the phenomenological and the folding model procedure due to different deformation of the imaginary parts. For sake of simplicity of the folding model calculations the deformation parameters of the nucleon distribution are taken as deformation parameters of $W(\vec{r}_\alpha)$. Some exploratory calculations with independent deformation indicate that this inconsistency just tends to increase the value of W_o (see Table 3).

5. ISOSCALAR TRANSITION RATES

Several procedures[9] have been worked out for deducing isoscalar transition rates

$$B(ISL, 0 \to L) = \left[\frac{Z}{A} \int \rho_L(r)\, r^{L+2}\, dr\right]^2 \qquad (5.1)$$

from alpha-particle scattering. The problem of explicit folding model calculations for extracting the transition density $\rho_L(r)$ can be bypassed by the analysis of radial moments (RMA) of the optical potential when exploiting the identity for folded potentials[22] (with a density independent

effective interaction)

$$\frac{\int U(\vec{r}_\alpha) r_\alpha^L Y_L^M(\hat{r}_\alpha) d^3r_\alpha}{\int U(\vec{r}_\alpha)\, d^3r_\alpha} = \frac{\int \rho(\vec{r}) r^L Y_L^M(\hat{r}) d^3r}{\int \rho(\vec{r})\, d^3r} \tag{5.2}$$

or written more specifically in terms of the results provided by the preceding analyses

$$\frac{\int V_L(r_\alpha)\, r_\alpha^{L+2}\, d\, r_\alpha}{J_0(V)} = \frac{\int \rho_L(r) r^{L+2} dr}{A} \tag{5.3}$$

There, the transition potential V_L of multipolarity L is just given by

$$V_L = \sum_t v_L^{(t)}(r_\alpha) \langle I || Q_L^{(t)} || I' \rangle \tag{5.4}$$

Table 4 compiles the obtained values derived with SW2 real form factors and compares the RMA procedure with the results of the explicit folding model analyses (where ρ_L is provided by derivatives of a Fermi distribution). The rates $G_L = B(ISL)/B_{sp}$ are given in single particle units using r_0=1.2 fm for the radius parameter. In the case of ^{90}Zr the values are compared to electromagnetic results[24] and the (α,α') result[25] extracted by a less reliable DWBA procedure (Bernstein procedure) from measurements at E_α = 31 MeV.

		RMA	Folding	Electromagn. ref. 24	BP-Proced. ref. 25
^{90}Zr	G_2	4.6 ± 0.4	3.5 ± 0.3	5.5 ± 0.5	5.7 ± 1.7
	G_4	1.7 ± 0.3	1.8 ± 0.3	3.3 ± 0.9	1.6 ± 0.2
^{92}Zr	G_2	4.4 ± 0.4	6.2 ± 0.5	-	-
	G_4	2.9 ± 0.3	2.4 ± 0.3	-	-

Table 4 Isoscalar quadrupole and hexadecapole transition rates G_L

6. CONCLUDING REMARKS

The present studies give some evidence that a squared Saxon-Woods shape is an improved parametrization not only for the elastic alpha-particle scattering potential (real part), but also for a deformed interaction potential the derivatives of which provide the transition potentials in inelastic scattering excitations. Of course, the problem remains, how to remove the model dependence due to the prechosen functional form of the form factors. There are recent attempts[23] to avoid such constraints by extending "model independent" procedures like the Fourier-Bessel method. For the particular cases studied ($0^+ - 2^+_1$ transitions in ^{50}Ti and ^{52}Cr), it turns out that "vibrational" form factors are quite well justified. If these results can be overtaken to the cases studied here, the RMA method should give quite reliable B(IS)-values as the unknown underlying effective interaction need not to be specified. It may be assumed to be rather complicated, composed of different components and also absorbing exchange effects. Strictly, such an implicit folding model interpretation is based on a density independent effective interaction. But it has been shown[14] that the influence of density dependence on the integral quantities like the volume integral J_0 is negligible. Due to the surface dominance, higher order radial moments should be affected even less.

A reliable determination of isoscalar transition rates is of considerable importance in view of possible differences of the deformation parameters for different transition mechanisms. This question has been discussed recently [26,27] and effects up to 25% might be expected, for single closed-shell nuclei and depending on the core-polarization of the nucleus considered. The case of hexadecapole transitions is of particular importance since alpha-particle scattering is most sensitive to that type of nuclear excitations. The present studies provide further evidence for hexadecapole motion in spherical and quasispherical nuclei, completing the systematics given in ref. 12. In general, there seems to be a considerable amount of (α,α') data indicating L=4 transitions. Unfortunately, due to lack of precision and due to the application of less certain methods of the analysis (like inadequate first-order calculations) many data are not adequate for a meaningful comparison. It is our feeling that the general problem is far to be solved, but the results of this paper can

be understood as a step towards an improved procedure and more accurate values of the transition probabilities.

The International Bureau, Kernforschungszentrum Karlsruhe, and the Central Institute of Physics have supported the collaboration. We are grateful to Professor Dr. G. Schatz and Professor Dr. M. Ivascu for their interest in these studies and acknowledge valuable discussions with Professor Dr. K. Grotowski. Dr. A. Ciocănel has participated in an early stage of the measurements.

REFERENCES

1) Proc. 2nd Louvain-Cracow Seminar: "The Alpha-Nucleus Interaction", eds. G. Gregoire and K. Grotowski, Universitê de Louvain, Belgium, June 5-7, 1978.

2) Goldberg, D.A., ref. 1, p. 41.
Gils, H.J., in "What do We Know about the Radial Shape of Nuclei in the Ca-Region?" Proc. Karlsruhe Int. Discussion Meeting, Karlsruhe, May 2-4, 1979, eds. H. Rebel, H.J. Gils, and G. Schatz KfK 2830 (1979).

3) Majka, Z., Gils, H.J., and Rebel, H., Z. Phys. A288 (1978) 139, Vinh Mau, N. Phys. Lett. 71B (1977) 5.

4) Friedman, E., and Batty, C.J., Phys. Rev. C17 (1978) 34.

5) Brissaud, I. and Brussel, M.K., J. Phys. 63 (1977) 481.
Roberson, P.L., Phys. Rev. C22 (1980) 482.

6) Put, L.W., and Paans, A.M.J., Nucl. Phys. A291 (1977) 93.

7) Budzanowski, A., Grotowski, K., Grzywacz, M. and Strzalkowski, A., Progr. Report Inst. of Nucl. Phys. Cracow (1972) unpublished.
Goldberg, D.A., Phys. Lett. 55B (1975) 59.

8) Majka, Z. and Srokowski, T., Acta Physica Polonica B9 (1978) 75.

9) Rebel, H., Z. Physik A277 (1976) 35.

10) Cowley, A.A. and Wall, N.S., Phys. Rev. C17 (1978) 1322.

11) Tamura, T., Progr. Theoret. Phys. Suppl. 37 und 38 (1966) 383.
Rebel, H., Löhken, R., Schweimer, G.W., Schatz, G., and Hauser, G. Z. Physik 256 (1972) 258.

12) Rebel, H., Gils, H.J. and Knüpfer, W., in Proc. XVI Int. Winter Meeting on Nuclear Physics, Bormio, Jan. 16-21, 1978, p. 532. ed. Iori, J., Inst. Fisica Universita, Milano, 1978.
Faust, H., Hanser, A., Klewe-Nebenius, H., Rebel, H., Buschmann, J., Gils, H.J., Journ. Phys. G: Nucl. Phys. 4 (1978) 247.

13) Gils, H.J., Friedman, E., Rebel, H., Buschmann, J., Zagromski, S. Klewe-Nebenius, H., Neumann, B., Pesl, R., and Bechtold, G. Phys. Rev. C21 (1980) 1239.

14) Friedman, E., Gils, H.J., Rebel, H., and Pesl, R. KfK 3038 (1980).

15) Gils, H.J., KfK 3063 (1980).

16) Budzanowski, A., Dabrowski, H., Freindl, L., Grotowski, K., Micek, S., Planeta, R., Strzalkowski, A., Bosman, M., Leleux, P., Macq, P., Meulders, J.P., and Pirat, C., Phys. Rev. C17 (1978) 951.

17) Schweimer, G.W. and Raynal, J., Private communication.
18) Rebel, H. and Schweimer, G.W., Z. Phys. 262 (1973) 59.
19) Rebel, H., Hauser, G., Schweimer, G.W., Nowicki, G., Wiesner, W., and Hartmann, D., Nucl. Phys. A218 (1974) 13.
20) Gils, H.J., Rebel, H., Buschmann, J., Klewe-Nebenius, H., Nowicki, G.P., and Nowatzke, W., Z. Phys. A249 (1976) 55.
21) De Jager, C.W., de Vries, H., and de Vries, C., Atomic Data and Nuclear Data Tables 14 (1974) 479, Academic Press, New York and London.
22) Satchler, G.R., J. Math. Phys. 13 (1972) 1118.
Mackintosh, R.S., Nucl. Phys. A266 (1976) 379.
23) Rebel, H., Pesl, R., Gils, H.J., Friedman, E., Nucl.Phys. A368 (1981) 61.
24) Endt, P.M., Atomic and Nuclear Data Tables 23, 6 (1979) 547.
25) Martens, E.J., Bernstein, A.M., Nucl. Phys. A 117 (1968) 24.
Phys. Lett. 24B (1967) 669.
26) Madsen, V.A., Brown, V.R., and Anderson, J.O., Phys. Rev. C12 (1975) 1205 - Phys. Rev. Lett. 34 (1975) 1398.
27) Bernstein, A.M., Brown, V.R., and Madsen, V.A., Phys. Lett. 103B (1981) 255 - Phys. Lett. 106B(1981) 259.